JJEES

JJEES (2019) 10 (3): 136-144
ISSN 1995-6681

Jordan Journal of Earth and Environmental Sciences

A GIS-based Hydrogeological and Geophysical Study for the Analysis of Potential Water Infiltration in the Upper Yarmouk River Basin, North Jordan

Muheeb Awawdeh[1*], Rasheed Jaradat[1], Khaldoon al Qudah[1], Nizar Abu-Jaber[2], Mohsen Awawdeh[3]

[1] *Yarmouk University, Department of Earth and Environment Sciences, Jordan*
[2] *German Jordanian University, Department of Civil and Environmental Engineering, Jordan*
[3] *King Faisal University, Department of Social Studies, Saudi Arabia*

Received 15 November 2018, Accepted 20 January 2019

Abstract

Groundwater resources in semi-arid climates in countries like Jordan have experienced deterioration both in quantity and quality. This paper aims at locating potential groundwater recharge areas in the Upper Yarmouk River Basin (UYRB) using weighted overlay method in ArcGIS. The input data for this analysis included geology, soil, land use/ land cover, slope, lineament density, and drainage density.

The results classified the study area in terms of its water infiltration potential into five categories, in which zones of high and very high infiltration potential represented 36 % of the investigated area. The maximum infiltration potential dominated the north, east, and southwest parts of the study. This is most probably due to the major influence of soil types, land cover and lineaments in the southwest, and the increased role of drainage density and topography in the north and eastern parts. The water infiltration potential was successfully validated using data from rainfall simulations and Vertical Electrical Soundings, suggesting that the moisture content of the upper 10m of the soil column is within the range 33-48%. The adopted model can be seen as a guide for water resources security and protection.

Keywords: Groundwater, Infiltration, Geographic Information System, Jordan.

1. Introduction

Water is one of the most essential commodities for mankind (Arkoprovo et al., 2012). Dominated by arid and semi-arid climates, Jordan suffers from a scarcity in natural water resources amid the increasing population growth. Economic developments and population increase have caused greater demand on water resources that resulted in a wide disparity between water supply and demand. In semi-arid regions, the partitioning of precipitation into surface runoff, infiltration and potential recharge are highly variable in space and time (Diiwu, 2004). It has been reported that about 93.9 % of the total rainfall in Jordan is lost and about 3.9 % only infiltrates to recharge the groundwater (Hadadin et al., 2010). Although the largest available source of fresh water in Jordan is obtained from groundwater, unsustainable practices of overdrawing put the water situation at risk in terms of quality and quantity (Odeh et al., 2019). Development and urbanization increase storm water runoff rates and volumes while decreasing infiltration. Moreover, climatic changes may provide even greater challenges in the future (Mohammad et el., 2018). Thus, water resources in Jordan need better management and protection strategies.

Infiltration occurs in areas where the permeability of the terrain, along with other factors, allows the rapid penetration of surface waters (Schneider et al., 2001). Part of this water percolates through the unsaturated zone of the soil and, and on reaching the water table, it recharges the aquifer. Groundwater recharge through infiltration is a very complex process which involves, but not limited to, rainfall, topography, soils, vegetation, climate, and land use (Al Kuisi and El-Naqa, 2013; Kahsay et al., 2018).

It has now become crucial to target recharge zones for artificial recharge in addition to identifying natural recharge zones in order to safeguard the water future. Artificial recharge is one of the effective techniques used for the management of groundwater resources (Raviraji et al., 2017). Ababneh (2013) found that the infiltration rate is increasing along an east -west transect in reference to soil characteristics across the Upper Yarmouk River Basin (UYRB). Al Qudah et al. (2015) have determined that the recharge rate in the UYRB ranges between 20 % and 37% of the amount of precipitation in contrast to other rates reported in previous studies (Bajjali, 2008; El -Naser, 1991; Water Authority of Jordan, 1989). Even the drier eastern areas of the basin show a notable evidence of the recharge in some areas (Abu-Jaber and Kharabsheh, 2008). This research is based on new findings (Ababneh, 2013; Al Qudah et al., 2015) and aimed at identifying the areas with the highest potential for surface water infiltration in the UYRB based on several key hydrogeological parameters.

* Corresponding author e-mail: awawdeh@yu.edu.jo

2. The Study Area

The study area is about 75 km2 (Fig. 1), with elevations ranging from 1,200 m in the highlands of Ajloun in the south down to 500 m west of the city of Ramtha in the north. Physiographically, the study area consists of the northern extension of the Ajloun highlands to the south and southwest, which grade into the Houran Plains to the north and northeast. Mediterranean climates dominate the southwest, receiving up to 600 mm/a of rain in the Ajloun highlands and around 470 mm/a in Irbid farther to the north. To the east, the climate becomes semi-arid to arid, and rainfall diminishes to about 215 mm/a in Ramtha and 150 mm/a in Mafraq (JMD, 2013). The rainfall is seasonal, falling mostly during the winter season over the months from October to April each year, with considerable annual rainfall variability. The main recharge area for the regional aquifer (B2/A7 Aquifer) is in the Ajloun highlands (Salameh, 2004). The northern end of the study area marks the start of Wadi Shallaleh, where groundwater discharges into Yarmouk River.

Geologically (Figure 2), the study area is dominated by the Upper Cretaceous Ajloun and Balqa Groups (Natural Resources Authority, 1993 and 1997). They consist of marine limestone, silicified limestone, marl and phosphorite formations. The Ajloun highlands are composed of the Upper Cretaceous limestones and dolostones that are largely karstified (Al Qudah et al., 2015). The Turonian Wadi Es Sir Formation (A7), with the overlying Campanian silicified limestone known as the Amman Formation (B2), makes up the major aquifer in the area known as the B2/A7. The Wadi Es Sir formation (Turonian) is a massive limestone formation that is highly karstified and the Amman formation (Santonian-Campanian) is a silicified limestone that has limited exposure in the northern extent of the Ajloun highlands. The southern part of the Houran Plains in Jordan are largely covered by soil which is underlain by the Muwaqqar Chalk Marl (MCM) Formation (B3). This formation (Maastrichtian) acts as an aquiclude because of the low permeability imparted by the marly clay layers creating a confined aquifer situation for the B2/A7 aquifer in that area. The Um Rijam Formation (B4) overlays the MCM Formation and consists of alternating chert and limestone beds. It acts as an aquifer in the Ramtha area, although its limited extent precludes it from being considered a regional water resource. The piezometric maps for the aquifer show a flow from the southwest towards the northeast, discharging at the springs of Wadi Shallaleh into the Yarmouk River. Although, the B2/A7 is generally viewed to obtain most of its recharge in the Ajloun Highlands, there is a strong isotopic evidence of recharge in the Nuymeh area (20 -25 km NE) as well (Bajjali, 2006). In addition, recharge has been identified farther to the east towards Mafraq (Abu-Jaber and Kharabsheh, 2008). This aquifer is the most important indigenous source of water in the Irbid Governorate (Bajjali, 2008).

Towards the east and northeast, flat plains, known as the Houran Plains, are spread with a thick red soil from the area which turns to a more yellow soil in the eastern reaches of the basin. The soils are Mediterranean red to brown soils, that consist of expandable clays (i.e. Montmorillonite). They tend to be thin in the higher area to the west and achieve thicknesses of several meters in the lower areas to the east (Al Qudah, 2015).

The study area is traditionally agricultural where olive groves, vineyards, and orchards are common in the Ajloun highlands, and crops such as wheat and barley are planted in the Houran Plains. These plains are gradually being converted for residential and commercial uses. Dense oak tree forests cover Ajloun highlands. However, about one fourth of the study area is urbanized, including mainly the cities of Irbid, Huson, Aidoon, Nuymeh, and Sareeh.

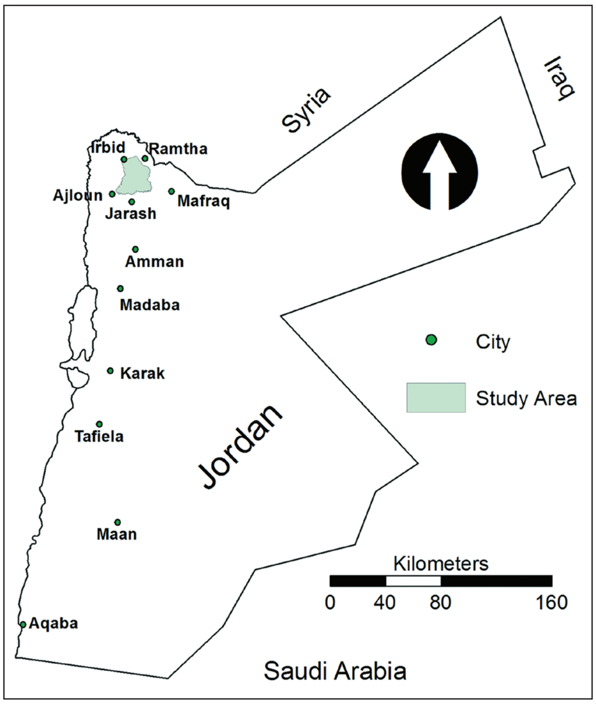

Figure 1. Location of the Upper Yarmouk River Basin, north Jordan.

3. Methods

Modeling areas with potential water infiltration is based on the concept of aquifer system contamination vulnerability. In other words, the most sensitive areas to the risk of contamination are the same areas of maximum infiltration, thus having the most favorable conditions for recharge of aquifer systems (Brito et al., 2006). Accordingly, the evaluation of areas with the highest infiltration must consider the hydrogeological characteristics of the terrain such as topography, land cover, and lineaments (Brito et al., 2006). Awawdeh and Jaradat (2010) evaluated the aquifers vulnerability to contamination in the Yarmouk River Basin. Many other studies assessed groundwater vulnerability to contamination in northern Jordan (Margane et al., 1999; Awawdeh and Nawafleh, 2008; Nawafleh et al., 2011, Awawdeh et al., 2015).

For this study, the proposed infiltration model is based on the selection and integration of information in a GIS system (ArcGIS 10.3). It combines several key hydrogeological parameters which describe the infiltration potential of present ground conditions.

Six hydrogeologyical parameters were taken into account to characterize the terrain infiltration potential including geology, soil, land cover, slope, lineaments, and drainage system. After data collection and editing, classes of each parameter were rated from 1 to 10 based on their relative effect on the infiltration capability, with rating 1 being the least infiltration potential and rating 10 being the highest. Different weights 1-5 (Table 1) were assigned to each parameter representing their relative importance in the conceptual infiltration model. Rates and weights were based on previous studiesand opinions of local experts.

It is well-established that GIS techniques can be successfully applied for the investigations of groundwater. Therefore, raster GIS layers of the hydrogeological parameters were algebraically combined in terms of weighted overlay methods to derive the potential infiltration model (Raviraji et al., 2017).

The model yields a numerical index that defines the variations in infiltration potential. The high infiltration potential index values define areas with maximum infiltration potential, while the low index values define little infiltration potential (impermeable areas). The final map has classified the study area into having very low, low, moderate, high, and very high infiltration capacities.

Table 1. Assigned weights for various hydrogeological parameters.

Parameters	Weights (1-5)
Soil	4
Land Use Land Cover	4
Geology	3
Slope	3
Drainage Density	3
Lineament Density	2

The next step was validating the groundwater potential model by using rainfall simulations (Al Qudah et al. 2015) and the near-surface geophysical technique (Vertical Electrical Sounding –VES). The aim of these tests was to develop a better understanding of the infiltration potential along model validation.

In this study, the geophysical investigation included eight vertical electrical soundings (VES) carried out using ARES GF-Instruments Resistivity meter adopting the Schlumberger electrode configuration. The VES points were located at different locations across a N-S profile (Figure 8). The prime goal was to investigate the electrical stratification and infiltration potential down to a depth of 10-15m along the investigated profile. Collected field data are given in Table 6. The Res1DINV inversion software (Loke, 2010) was used for data inversion of the observed apparent resistivity values, where the inversion process was carried out assuming no specific initial inversion model, in that the software was allowed to use the same number of layers and thicknesses to allow for a valid comparison between the investigated points. The root mean square was used as a measure of fit.

To check the validity of the modeled infiltration potential, the value of soil moisture-content was estimated from electrical resistivity values and laboratory-based experiments using linear or non-linear regression analyses (Ozcep et al. 2009; Bahatt et al., 2014; Kazmi et al., 2016).

4. Results and Discussion

4.1 The Physical Conditions of the Basin

Figure 2 shows the detailed geology of the study area. The study area is dominated by Wadi Es Sir Formation in the southern parts (29 %), and by Amman Silicified Limestone in the middle (18 %). Soil dominates (41%) the northern part of the basin. The rating values for each formation (Table 2) were assigned based on the general characteristics of each formation.

The soil map (Figure 3) was modified after the National Soil Map and Land Use project (Ministry of Agriculture, 1994). The available data were processed and evaluated to extract appropriate information on soil texture. It is believed that more details are required to yield a more accurate soil-texture map; therefore, data from recent studies (Ababneh, 2013; Al Qudah et al., 2015) were also considered to reflect more accurate soil-texture properties. Accordingly, most of the area is dominated by silt loam and sandy soils. Table 3 lists the rating values of each soil type.

The land use/ land cover (LULC) map was digitized from Google Earth. There are six main classes of LULC in the area: agriculture, bareland, forest, orchard (mainly olive), rangeland, and urban (Figure 4). Table 4 shows the area coverage for each LULC class and its rating value. Most of the area is occupied by either rangeland (30 %), agriculture (24 %), urban (18 %), or orchard (17 %).

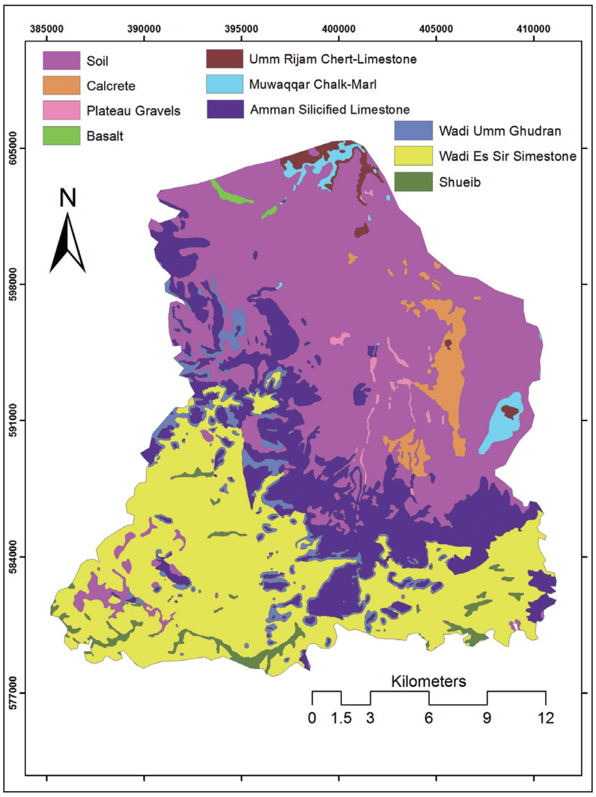

Figure 2. Geology of the upper part of the Upper Yarmouk River Basin (modified after the Natural Resources Authority, 1993 and 1997).

Table 2. Rating values of the geology map.

Formation	Rating value	Area Coverage (%)
Soil	6	41.19
Calcrete	1	2.68
Plateau Gravels	8	0.58
Basalt	7	0.23
Umm Rijam Chert-Limestone	5	0.92
Muwaqqar Chalk-Marl	3	1.28
Amman Silicified Limestone	6	18.37
Wadi Umm Ghudran	4	3.97
Wadi Es Sir Limestone	6	29.29
Shueib	3	1.50

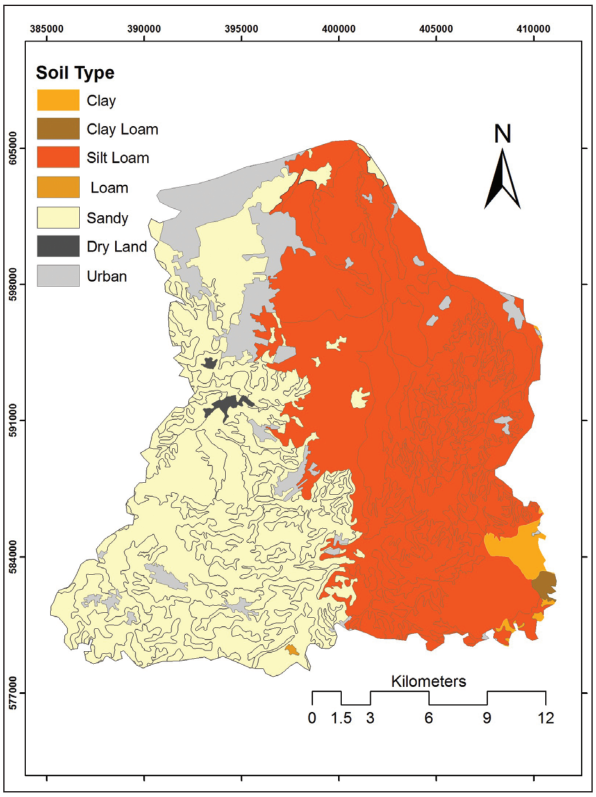

Figure 3. Soil types of the upper part of the Upper Yarmouk River Basin (modified after the Ministry of Agriculture, 1994).

Table 3. Ratings of the soil types in the upper part of the Yarmouk River Basin.

Soil Type	Rating value
Clay	3
Clay loam	2
Silt Loam	5
Loam	5
Sandy	7
Bareland	2
Urban	2

The topographic maps (1:50,000) of the Natural Resources Authority (1993 and 1997) were digitized and interpolated in GIS to derive the digital elevation model for the study area. Generally, the elevations are decreasing towards the north. A slope map (Figure 5) was derived and assigned rating values as shown in Table 5. The slope ranged from flat areas mainly in the east to 60° in the highlands. The lineaments density was calculated, classified, and rated as showed in Figure 6. The surface lineaments mapped here are those linear features observed on satellite images from Google Earth and are believed to concentrate recharge and flow. The density of lineaments is highest in the south western part of the study area, where slope is greater.

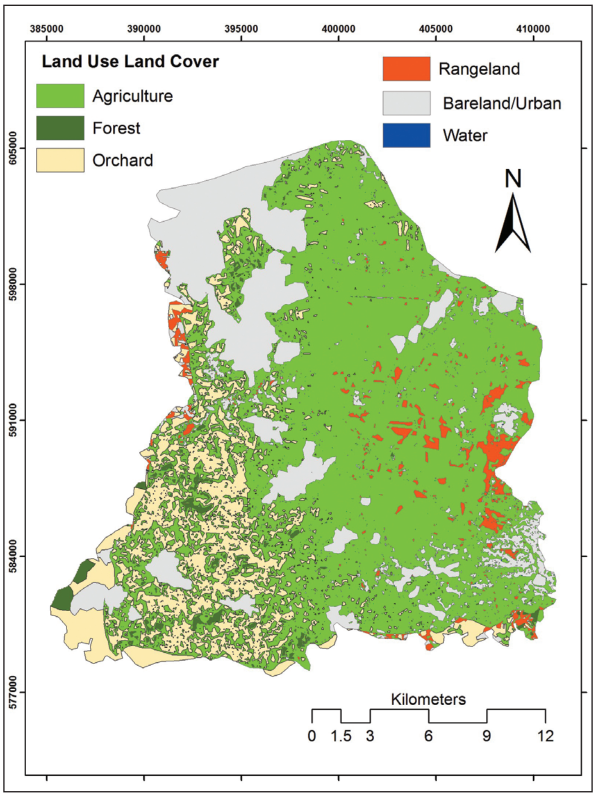

Figure 4. Land use/ land covers in the upper part of the Upper Yarmouk River Basin.

Table 4. Ratings of the land use/ land cover in the upper part of the Yarmouk River Basin.

Class	Rating Value	Area Coverage (%)
Agriculture	6	24.12
Bareland	3	1.81
Forest	9	7.63
Orchard	7	17.43
Rangeland	5	30.57
Urban	3	18.14

Table 5. Rating of slopes in the upper part of the Yarmouk River Basin.

Topography (C) %	Rating
0-2	1
3-4	2
5-6	3
7-9	4
10-12	5
13-15	6
16-18	7
19-21	8
22-25	9
>25	10

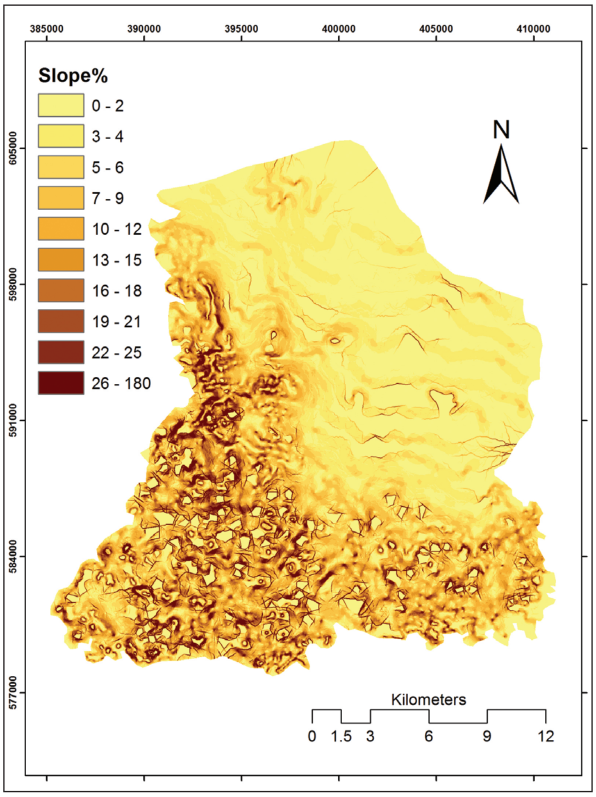

Figure 5. Topography of the upper part of the Upper Yarmouk River Basin.

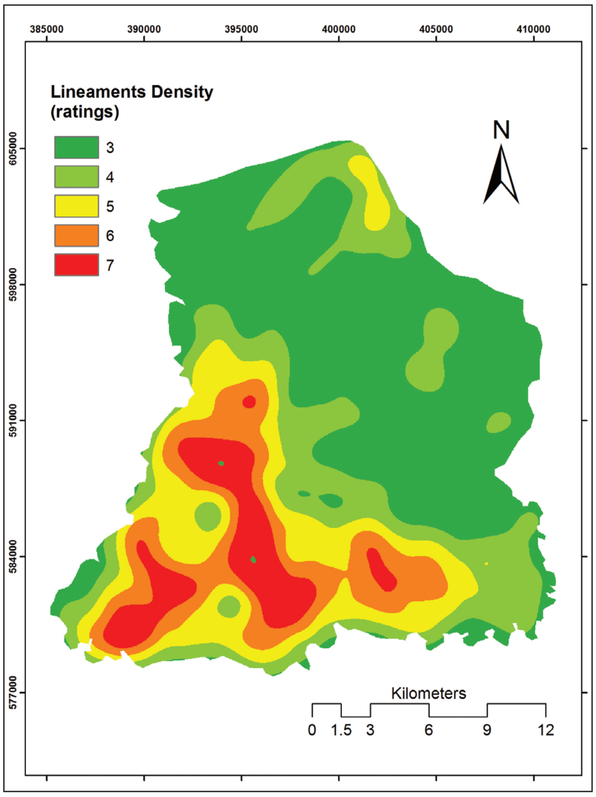

Figure 6. Ratings' map of the lineaments density in the upper part of the Yarmouk River Basin.

Images from Google Earth were also the source data to map the drainage network. The drainage density map was calculated, classified and rated appropriately (Figure 7). Drainage density was highest in the east; close to Wadi Nuymeh in the east and to Wadi Shalaleh in the north.

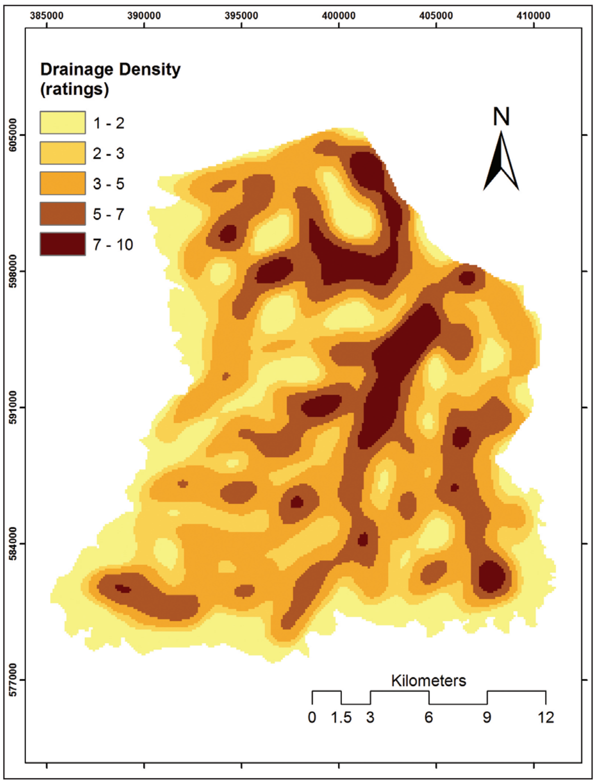

Figure 7. Drainage density rating of the upper part of the Yarmouk River Basin.

4.2 Mapping of the Potential Infiltration Areas

After successful integration of all the thematic maps, an output raster map was obtained indicating the zones with potential infiltration. The infiltration potential index was reclassified into five categories (Figure 8): very low (9.30 %), low (24 %), moderate (30.60 %), high (26.37 %) and very high (9.70 %).

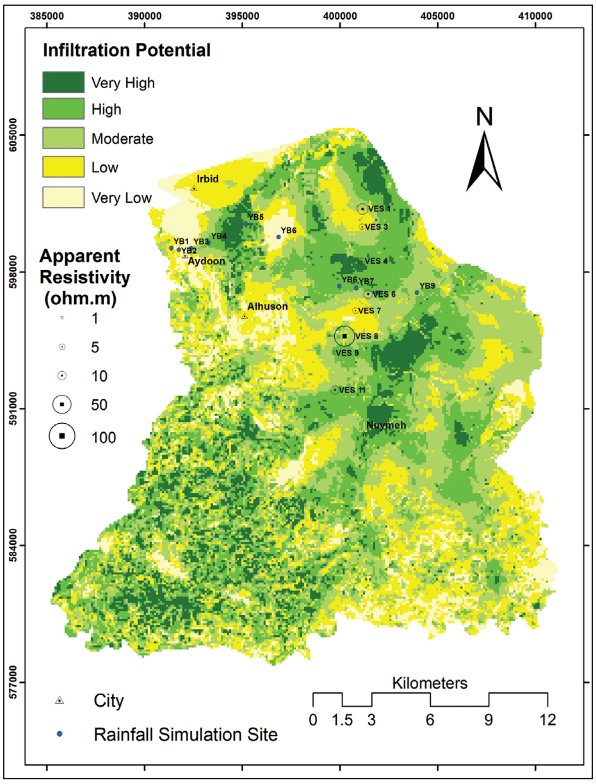

Figure 8. Potential infiltration of the upper part of the Upper Yarmouk River Basin.

Most of the areas in the high infiltration potential category are found along a southwest northeast axis and in the eastern parts of the study area. This can be attributed to the role of soil types, land cover, and lineaments in the southwest, and to the role of drainage density and topography in the north and eastern parts. About 36 % of the study area is categorized into having a high to very high infiltration potential.

4.3 Model Validation

Data from experimental rainfall field simulations (Al Qudah et al., 2015), in addition to geophysical field investigations (Vertical Electrical Soundings) were processed and used to validate the results of the infiltration potential index map (Figure 8).

Rainfall field simulations proved that water in the area penetrates the soil quickly with relatively little runoff (Al Qudah et al., 2015). The loss of moisture through the summer months occurs more likely through the drainage to deeper zones (recharge) than from evaporation. This is verified by the lack of soil carbonate accumulation in most of the soils in the area (Al Qudah et al., 2015).

The results of the inversion process are illustrated in Figure 9, indicating a variable electrical stratification. Several low electric resistivity values were encountered, almost in all of the investigated VES locations, suggesting wet conditions from potential groundwater local infiltration processes. This conclusion was valid for all of the investigated points except resulting in elevated resistivity values. A weighted average resistivity value representing the first 10m of each VES point was calculated (Table 7), using the following equation:

$$Average\ Res._{10m} = \frac{\mathbf{10}}{\sum_{i=1}^{n}\left(\frac{h}{\rho_i}\right)} \text{ ....eq.(1)}$$

where h is the thickness of each resistivity layer, and ρi is the resistivity of that layer.

Figure 8 illustrates the comparison between the posted average inverted resistivity values for the upper 10m and the potential infiltration map, suggesting a good fit (70 %) between the infiltration potential classes and the computed average resistivity values. Al Qudah et al. (2015) described the soil of the study area as a silty-silty loam soil type with the soil-moisture content variying between 18-27 % for the upper 1m of the soil column. However, it is expected that the moisture content increases with depth due to increased water retention as deeper sections of soil and weathered bedrock material were approached. Nusier and Alawneh (2002) presented a water moisture-content variation with depth and seasonality variations of selected uncovered soil locations down to a depth of 10m, indicating that water content ranges between 20 % and 40%. Additionally, they showed that the depth of the zone of seasonal moisture-content variation is at about 3 m, below, and the moisture content tends to increase with depth (Figure 10).

Table 6. Field results of vertical electrical sounding (VES).

	AB/2	MN/2	Apparent Resistivity (ohm.m)							
	(m)	(m)	VES 1	VES 3	VES 4	VES 6	VES 7	VES 8	VES 9	VES 11
1	1	0.2	6.24	13.57	23.09	11.35	14.74	8.69	13.68	8.39
2	1.3	0.2	5.65	13.07	21.63	10.31	14.29	10.9	6.68	7.17
3	1.7	0.2	6.5	13.93	23.63	8.69	11.75	13.84	7.51	7.46
4	2.2	0.2	7.84	14.05	19.89	8.43	10.44	17.87	3.3	7.23
5	2.8	0.2	7.31	11.42	19.04	9.01	7.99	22.55	3.46	7.31
6	3.7	0.2	9.92	9.05	11.81	8.72	6.4	30.4	3.21	6.5
7	4.7	0.2	10.92	8.21	10.52	10	5.59	39.2	2.88	7.12
8	3.7	1	17.2	9.62	12.24	14.04	6.63	30.87	4.3	6.54
9	4.7	1	20.53	8.5	10.79	16.04	5.61	40.7	3.77	7.12
10	6.1	1	25.08	7.1	9.13	18.15	5.23	49.95	3.87	8.02
11	8	1	29.76	6.47	8.13	19.4	5.42	63.06	3.97	9.48
12	10.3	1	34.63	6.37	8.2	21.6	6.02	73.24	4.35	11.9
13	13.4	1	39.19	6.11	8.5	24.25	7.16	94.6	5	12.69

It would be a valid assumption to check the validity of the modeled infiltration potential, if a general estimate for the value of soil moisture-content within the soil column is given based on estimated resistivity values. Several studies investigated the potential to estimate the moisture of soil-water content from electrical resistivity values from field VES and laboratory-based experiments using linear or non-linear regression analyses (Ozcep et al. 2009; Bahatt et al., 2014; Kazmi et al., 2016). Some of these equations were developed assuming general types of soil, while other equations were developed for specific types such as sandy or silt-sand soils. Table 8 presents the estimated moisture contents using the Average Res. 10m values. Comparing the estimated results with those presented by Al Qudah (2015) and Nusier and Alawneh (2002), it can be said that the models of silty-sand (Kazmi et al., 2016) and all soil types (Ozcep et al., 2009) correlate well with the soils of the study area, suggesting a moisture content within the range of 33-48%. However, soil samples from a location within a close distance to the rock outcrops (i.e. VES-8) showed very low moisture-content values (15%).

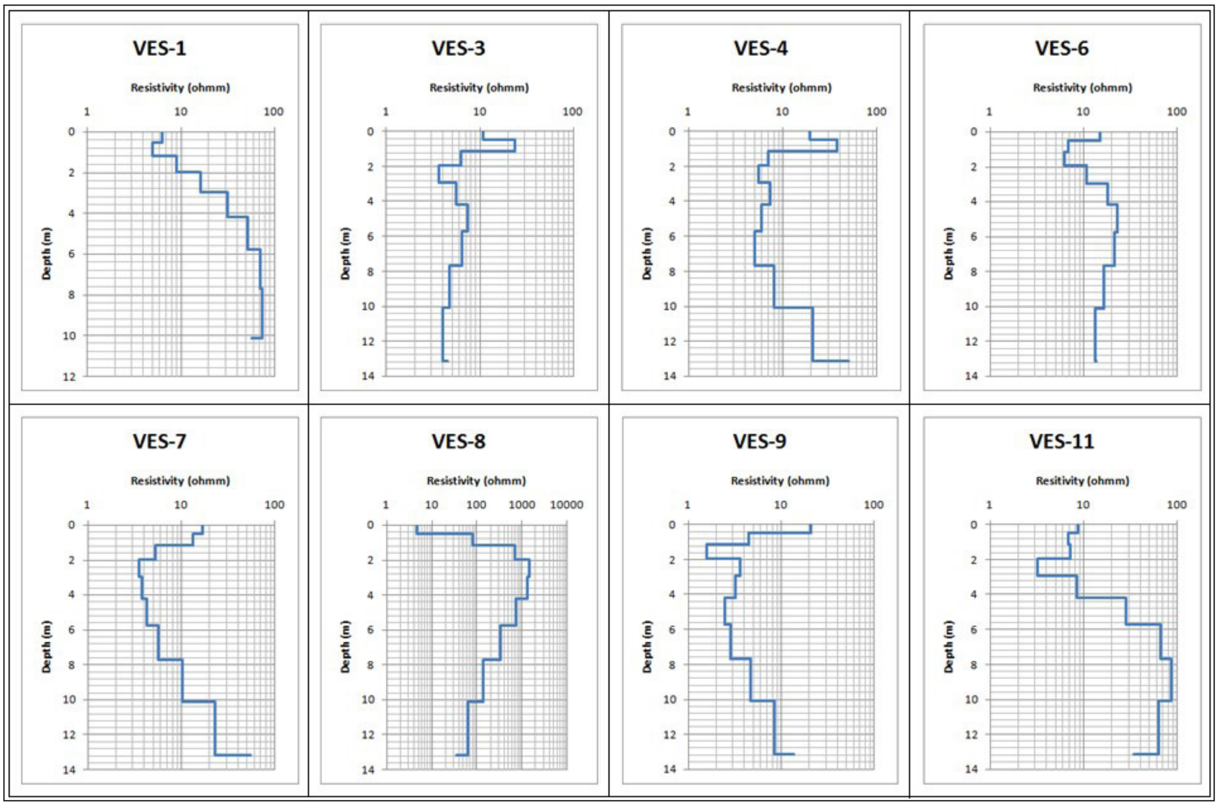

Figure 9. 1D inversion results of the collected Vertical Electrical Resistivity.

Table 7. Average resistivity values (Average Res.$_{10m}$) estimated for the upper 10m.

No.	ID	Average Res.$_{10m}$ (Ohm.m)
1	VES-1	20.86
2	VES-3	5.9
3	VES-4	6.99
4	VES-6	14.04
5	VES-7	5.65
6	VES-8	70.18
7	VES-9	3.17
8	VES-11	12.24

Table 8. Estimated moisture content using Average Res.$_{10m}$ based on several regression models. ([1]Bahhat et al. (2014), [2]Kazmi et al. (2016), [3]Ozcep et al. (2009)).

No.	ID	Estimated Moisture Content (%)			
		Sand[1]	All Soil[2]	Sity-sand soil[2]	All soil types[3]
1	VES-1	26.06	42.02	39.00	34.52
2	VES-3	28.51	58.43	44.87	44.51
3	VES-4	28.32	55.90	44.08	43.70
4	VES-6	27.15	46.60	40.84	38.76
5	VES-7	28.55	59.10	45.07	44.70
6	VES-8	19.39	30.62	33.37	14.92
7	VES-9	28.98	68.72	47.75	46.63
8	VES-11	27.44	48.30	41.48	39.97
Minimum:		19.4	30.6	33.4	14.9
Maximum:		29.0	68.7	47.8	46.6
Average:		26.8	51.2	42.1	38.5

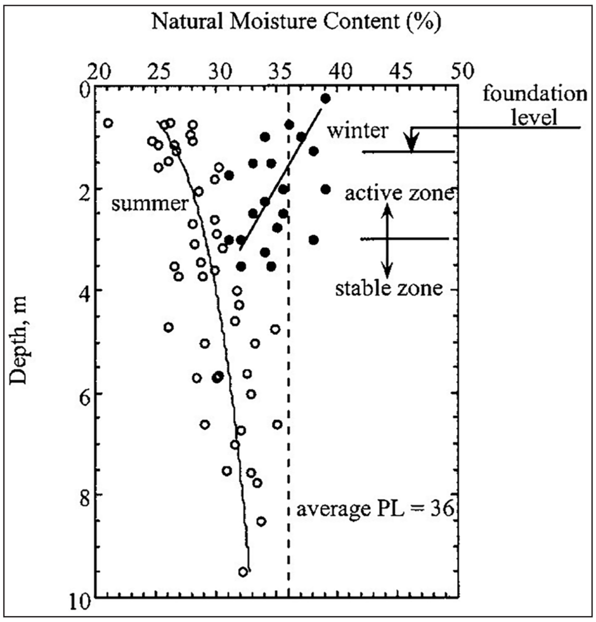

Figure 10. Seasonal variation of natural moisture content with depth of several locations representing uncovered Irbid soil samples (Nusier and Alwaneh, 2002).

5. Conclusions

The approach adopted by the current study has enabled the mapping of areas with potential water infiltration in a very important basin in northern Jordan. The combination of several essential hydrological parameters into a final map summarizes the most favorable conditions for recharging aquifer systems, and provides important strategic information as well for the location of priority protection areas because of the vulnerability of the aquifer to potential contamination. The water infiltration potential was successfully validated using data from rainfall simulations and geophysical surveying, suggesting that the moisture content of the upper 10m of the soil column is within the range of 33-48 %.

With increasing urbanization, there would be fewer areas available to storm water for infiltration. This model can be seen as a guide for water resources' security and protection strategies against the vulnerability of the aquifers and for land-use planning. Priority protection areas (high potential infiltration areas) must be considered seriously by the decision-making authorities. The authors suggest installing various groundwater recharge structures like boulder dams, check dams, percolation tanks, recharge pits etc., in appropriate locations to ensure high amounts of groundwater recharge.

Acknowledgments

We would like to thank the Jordanian Scientific Recearch Fund for their generous support of this project (3/2008).

References

Ababneh, E. (2013). Spatial variations in soil properties and infiltration rate in top soil a long a semi-arid transect, North Jordan. MSc thesis Yarmouk University, Irbid.

Abu-Jaber, N., and Kharabsheh, A. (2008). Ground water origin and movement in the upper Yarmouk Basin, Northern Jordan. Environmental geology, 54(7): 1355-1365.

Al Kuisi, M., and El-Naqa A. (2013). GIS based spatial groundwater recharge estimation in the Jafr basin, Jordan-application of wetspass models for arid regions. Rev Mex Cienc Geol, 30(1): 96–109.

Al Qudah, K., Abu-Jaber, N., Jaradat, R., Awawdeh, M. (2015). Artificial rainfall tests, soil moisture profiles and geoelectrical investigations for the estimation of recharge rates in a semi-arid area (Jordanian Yarmouk River Basin). Environmental Earth Sciences, 73: 6677–6689.

Arkoprovo, B., Adarsa, J, Prakash, S. (2012). Delineation of groundwater potential zones using satellite remote sensing and geographic information system techniques: a case study from Ganjam district, Orissa, India. Res. J. Recent Sci., 1(9): 59–66.

Awawdeh, M., Obeidat, M., Zaiter, G. (2015). Groundwater Vulnerability Assessment in the Vicinity of Ramtha Wastewater Treatment Plant, North Jordan. Applied Water Science, 5: 321–334.

Awawdeh, M., and Jaradat, R. (2010). Evaluation of Aquifers Vulnerability to Contamination in the Yarmouk River Basin, Jordan, Based on DRASTIC Method. Arabian Journal of Geosciences, 3(3): 273-282.

Awawdeh, M., and Nawafleh, A. (2008). A GIS -based EPIK Model for Assessing Aquifer Vulnerability in Irbid Governorate, North Jordan. Jordan Journal of Civil Engineering, 2(3): 267-278.

Bajjali, W. (2008). Evaluation of groundwater in a three-aquifer system in Ramtha area, Jordan: recharge mechanisms, hydraulic relationship and geochemical evolution. Hydrogeol. Journal, 16: 193–1205

Bhatt, S., and Jain, P. (2014). Correlation between electrical resistivity and water content of sand – a statistical approach. American International Journal of Research in Science, Technology, Engineering and Mathematics, 6(2): 115-121.

Brito, M., Costa, C., Almeida, J., Vendas, D., Verdial, P. (2006). Characterization of maximum infiltration using GIS tools. Engineering Geology, 85:14–18.

Diiwu, J. (2004). Groundwater-surface water interaction as a component of the ecohydrology of semi-arid regions. J. Environment systems, 30(2): 91-104.

El-Naser, H. (1991). Groundwater of the deep aquifer systems in NW Jordan: hydrogeological and hydrogeochemical quasi 3-D modeling. PhD Thesis, University of Wurzburg.

Hadadin, N., Qaqish, M., Akawwi, E., Bdour, A. (2010). Water shortage in Jordan— Sustainable solutions. Desalination, 250: 197–202.

JMD (Jordan Meteorological Department). Website. http://www.jmd.gov.jo. (2013). Accessed 2 Feb 2013.

Kahsay, G., Gebreyohannes, T., Gebremedhin, M., Gebrekirstos, A., Birhane, E., Gebrewahid, H., Welegebriel, L. (2018). Spatial groundwater recharge estimation in Raya basin, Northern Ethiopia: an approach using GIS based water balance model. Sustainable Water Resources Management.

Kazmi, D., Qasim, S., Siddiqui, F., Azhar, S. (2016). Exploring the Relationship between Moisture Content and Electrical Resistivity for Sandy and Silty Soils. International Journal of Engineering Science Invention, 5(6): 33-35.

Loke, M. (2010). RES1D version 1.00.08, 1-D resistivity, IP and SIP inversion and forward modeling, Geotomo software, https://www.geoelectrical.com.

Margane, A., Hobler, M., Subah, A. (1999). Mapping of groundwater vulnerability and hazards to groundwater in the Irbid Area, N Jordan. Z Angew Geol, 45(4): 175–187.

Ministry of Agriculture. (1994). The soils of Jordan. National Soil Map and Land Use project. Hunting Technical Services Ltd, and Soil Survey and Land Research Center, Amman, Jordan.

Mohammad, A., Jung, H., Odeh, T., Bhuiyan, C., Hussein, H. (2018). Understanding the impact of droughts in the Yarmouk Basin, Jordan: monitoring droughts through meteorological and hydrological drought indices. Arabian Journal of Geosciences, 11(5): 103.

Natural Resources Authority. (1997). Geological Map of Irbid 3155 II, sheet No.15. Geology Directorate, Amman.

Natural Resources Authority. (1993). Geological Map of Jerash 3154 I, sheet No.27. Geology Directorate, Amman.

Nawafleh, A., Awawdeh, M., Salameh, E. (2011). Assessment of Groundwater Vulnerability to Contamination in Irbid Governorate, North Jordan. DIRASAT, 38(2).

Nusier, O., and Alawneh, S. 2002. Damage of Reinforced Concrete Structure due to Severe Soil Expansion, Journal of Performance of Constructed Facilities, 16(1): 33-41.

Odeh, T., Mohammad, A., Hussein, H., Ismail, M., Almomani, T. (2019). Over-pumping of groundwater in Irbid governorate, northern Jordan: a conceptual model to analyze the effects of urbanization and agricultural activities on groundwater levels and salinity. Environmental Earth Sciences, 78(1): 40.

Ozcep, F., Tezel, O., Asci, M. (2009). Correlation between electrical resistivity and soil-water content: Istanbul and Golcuk. Int. J. Phys. Sci., 4(6): 362–365.

Raviraj, A., Kuruppath, N., Kannan, B. (2017). Identification of Potential Groundwater Recharge Zones Using Remote Sensing and Geographical Information System in Amaravathy Basin. Journal of Remote Sensing and GIS, 6:4.

Salameh, E. (2004). Using environmental isotopes in the study of the recharge-discharge discharge mechanisms of the Yarmouk catchment area in Jordan. Hydrogeol. J. 12: 451–463

Schneider, M., Forrest, I., Wallis, G., Maclean, B., Beukeboom, T., Armstrong, B., Leach, R.; Simpson, H., Graul, P., Armstrong, C., Salter, J., Grant, B., Schmidt, M., Hern, D., Teahen, G., Bateman, D., Reid, S. (2001). Perth County Groundwater Study – Final Report– Upper Thames River Conservation Authority, Ausable–Bayfield Conservation Authority, Maitland Valley Conservation Authority.

Water Authority of Jordan (WAJ) (1989) North Jordan water resources investigation project. Yarmouk basin water resources study final technical report, Amman